Journal of Solid State Chemistry 182 (2009) 862–868

Contents lists available at ScienceDirect

Journal of Solid State Chemistry

journal homepage: www.elsevier.com/locate/jssc

Uniform silica nanoparticles encapsulating two-photon absorbing fluorescent dye

Wei-Bing Wu [a,b], Chang Liu [c], Ming-Liang Wang [a,*], Wei Huang [c], Sheng-Rui Zhou [a], Wei Jiang [a], Yue-Ming Sun [a], Yi-Ping Cui [c], Chun-Xinag Xu [c]

[a] School of Chemistry and Chemical Engineering, Southeast University, Nanjing 211189, PR China
[b] School of Light-Industry Science and Engineering, Nanjing Forestry University, Nanjing 210037, PR China
[c] Advanced Photonics Center, School of Electronic Science and Engineering, Southeast University, Nanjing 210096, PR China

ARTICLE INFO

Article history:
Received 14 December 2007
Received in revised form
28 November 2008
Accepted 14 December 2008
Available online 24 December 2008

Keywords:
Silica nanoparticles
Two-photon excited fluorescence
Solvent effect
Reverse microemulsion

ABSTRACT

We have prepared uniform silica nanoparticles (NPs) doped with a two-photon absorbing zwitterionic hemicyanine dye by reverse microemulsion method. Obvious solvatochromism on the absorption spectra of dye-doped NPs indicates that solvents can partly penetrate into the silica matrix and then affect the ground and excited state of dye molecules. For dye-doped NP suspensions, both one-photon and two-photon excited fluorescence are much stronger and recorded at shorter wavelength compared to those of free dye solutions with comparative overall dye concentration. This behavior is possibly attributed to the restricted twisted intramolecular charge transfer (TICT), which reduces fluorescence quenching when dye molecules are trapped in the silica matrix. Images from two-photon laser scanning fluorescence microscopy demonstrate that the dye-doped silica NPs can be actively uptaken by Hela cells with low cytotoxicity.

1. Introduction

Nanoparticles (NPs) show many unique properties, such as optical, electrical, magnetic, and chemical, which are not observed in the bulk material. There is widespread academic and commercial interest in incorporation of dyes within silica NP matrixes [1–5]. For example, they have accelerated the development of fluorescent probes that have applications in bioanalytical, biotechnological, and biomedical fields [6–9]. Among the great variety of dyes available for inclusion in functional NPs, two-photon absorbing (TPA) fluorescent dyes have gained increasing relevance for applications in the bio-imaging field [10,11].

TPA bio-imaging is a non-invasive, non-destructive technique that employs near IR light (usually in the 700–1000 nm range), which allows deeper penetration of the tissues and low scattering of the excitation beam, as pumping source. Moreover, the highly spatially localized excitation can improve three-dimensional resolution [12]. A useful TPA probe for such applications should have strong fluorescence signal in aqueous media, appreciable water solubility, cell permeability, high photostability, biocompatibility, and low toxicity. Many research efforts are focusing on the development of useful fluorophores [13–15]. However, most of these fluorophores are hydrophobic and often require multistep synthesis. For the few hydrophilic fluoreophores, their fluorescence quantum yields are usually reduced to a considerable extent in water because of solvent effect [16]. Silica-based NPs containing TPA dye is a valuable alternative to pristine dyes. In fact, dye-doped NPs are biocompatible encapsulating carriers with an overall improvement of performance compared to the isolated dye molecules, such as intense fluorescence signal, minimized photobleaching, simple surface modification, and low toxicity etc. [17].

Quite scarce researches, however, have been focused on the silica NPs doped with fluorescent dyes optimized for two-photon absorption and fluorescence. Prasad and co-workers have prepared composite silica NPs loaded with TPA dyes and studied their potential applications [18–21]. Bertazza et al. also reported the preparation and properties of organosilica NPs doped with TPA fluorophores of the distyrylbenzene class [22]. Solvent resistance of dye-doped silica NPs is important since stable fluorescence signals are usually required for biological assays and detections. In addition, silica NPs may need further modification for practical application and they must withstand harsh solvents (e.g. acetonitrile, dimethylformamide (DMF), dimethylsulfoxide (DMSO)) that may be used in the potential synthetic routes [23]. However, few researches have been focused on the solvent effect on the optical properties of dye-doped silica NPs. In this paper, we have prepared silica NPs containing a TPA fluorophores 4-[2-(4-diphenylamino-phenyl)-vinyl]-1-methyl-pyridinium iodide (DPPI) [24] and made detailed research about the solvent effect on their

* Corresponding author. Fax: +86 25 83795821.
E-mail address: wangmlchem@263.net (M.-L. Wang).

0022-4596/$ - see front matter © 2009 Elsevier Inc. All rights reserved.
doi:10.1016/j.jssc.2008.12.003

absorption, one-photon excited (OPE), and two-photon excited (TPE) fluorescence properties in various solvents. The synthesis of such DPPI-doped composite NPs (DPPI-NPs) is achieved by carrying out reaction within a reverse micellar cavity [25]. We have also demonstrated their potential application in TPA bioimaging.

2. Experimental

2.1. General

Triton X-100 was purchased from Sigma. Commercially available tetraethyl orthosilicate (TEOS), $NH_3 \cdot H_2O$ (28.0–30.0%) and *n*-hexanol were used as received. All the solvents were of analytical grade and used without further purification. DPPI was supplied by Liu and was synthesized as described by Wang [24]. Its structure was identified by ^{1}H NMR and Element analysis. ^{1}H NMR (CD_3OD, 300 MHz) δ: 8.62–8.64 (d, 2H, $J = 6.66$ Hz), 8.07–8.09 (d, 2H, $J = 6.69$ Hz), 7.85–7.91 (d, 1H, $J = 16.14$ Hz), 7.60–7.63 (d, 2H, $J = 8.67$ Hz), 7.33–7.39 (m, 4H), 7.23–7.28 (d, 1H, $J = 16.17$ Hz), 7.13–7.19 (m, 6H), 6.99–7.02 (d, 2H, $J = 8.64$ Hz), 4.29 (s, 3H). Anal. calcd. for $C_{26}H_{23}N_2I$: C, 63.68; H, 4.73; N, 5.71. Found: C, 63.60; H, 4.89; N, 5.66.

The size and morphology of NPs were measured using a transmission electron microscope (Hitachi H-600) at an operating voltage of 120 kV. The samples for transmission electron microscopy (TEM) were prepared by placing a dilute aqueous dispersion on 200 mesh carbon-coated copper grids. Dimensional analysis of NPs was made using *ImageJ* software.

Absorption spectra were observed on a Shimadzu model UV-2201 UV–vis spectrophotometer using a quartz cuvette (1-cm path length). The OPE fluorescence spectra were recorded on a FLS-920 fluorescence spectrophotometer (Edinburgh Instruments Ltd.) with a xenon arc lamp as the excitation source. All the OPE fluorescence measurements were conducted under the same conditions.

The excitation source used for TPE fluorescence was a Ti: sapphire oscillator/amplifier producing ~150 fs duration, 800-nm-wavelength laser output with a repetition rate of 1 kHz. After focused by 10-cm lens, the laser beam was guided into the sample cell and the emission was collected by 0.3-m triple grating monochromator/spectrograph through optical fiber detector at 90° geometry.

2.2. Preparation of the DPPI-NPs

In a typical quaternary microemulsion system for preparation of silica NPs using Trition X-100 as surfactant, a water-in-oil microemulsion was prepared by mixing 3.54 mL of Triton X-100, 15 mL of cyclohexane, 3.6 mL of *n*-hexanol, and 0.1 mL dye aqueous solution containing 1.8 mg DPPI. TEOS of 200 μL was then added as a precursor for silica formation, followed by addition of 200 μL $NH_3 \cdot H_2O$ to initiate the polymerization process. The reaction was allowed to continue for 24 h at room temperature followed by addition of acetone to break the microemulsion and recover the particles. In order to remove the attached surfactant and free dye, the resulting NPs were purified by successively washing with chloroform, acetone and ethanol. Afterwards, they were dried in vacuum at room temperature. The suspension samples for spectrum measurements were prepared by ultrasonic dispersing for 5 min. Then the suspensions were adjusted at pH 9 by addition of aqueous ammonia to introduce a negative charge on the surface of silica NP, which can prevent aggregation by electrostatic repulsion.

2.3. NP uptake and imaging

Hela cells purchased from Nanjing Kaiji Biotechnology Co. Ltd. were thawed, washed with a high glucose Dulbecco's modified Eagle's medium (DMEM, Sigma-Aldrich), seeded out in culture dishes (Corning). Cells were then grown for 24 h in DMEM supplemented with 10% calf serum in a 5% CO_2 cell culture incubator at 37 °C with 95% relative humidity. At 2 h prior to experiments, the culture medium was replaced by a culture medium mixed with 0.2 mg/mL DPPI-NPs aqueous dispersions. Internalization of the DPPI-NPs occurred by fluid phase uptake from the culture medium. Fluorescence images were obtained by OLYMPUS FluoView^{TM} FV1000 laser confocal scanning microscopy. The light at 800 nm from a Ti: sapphire fs laser (Mira Optima 900-F) was employed for TPE fluorescence images. The average input power of the femtosecond laser was 31 mW and FWHM was adjusted to 10.8 nm. A 60 × oil immersion microscope objective was used to focus the excitation beam to a diffraction-limited spot on the sample surface. Scan range was 70.4 μm × 52.3 μm and scan speed was selected as 10 μs/pixel.

2.4. Cell viability assay

The cytotoxicity of DPPI-NPs was tested using an in vitro MTT (3-[4,5-dimethylthiazol-2-yl]2,5-diphenyl tetrazolium bromide) based assay kit (Sigma). In this method, formazan crystals (produced by the cleavage of MTT by dehydrogenases in living cells) are dissolved in acidified isopropanol and the solution is spectrophotometrically measured at 570 nm. The cells were seeded in 96 multi-well plates (3.0×10^4 cells/well) and incubated with a suspension of DPPI-NPs in a humidity incubator with 5% CO_2 at 37 °C for 2 h. After treatment, MTT solution was added and the cells were incubated following the supplier indications. The optical densities at 570 nm were used to determine the viability of cell.

3. Results and discussion

3.1. Preparation and characterization of DPPI-NPs

The inclusion of dye into silica NPs was performed using reverse microemulsion method. Trition X-100 and *n*-hexanol were used as surfactant and cosurfactant, respectively. Polymerization of TEOS takes place in the polar core of Triton X-100 micells, which also incorporate the dye, and results in the formation of dye-doped NPs. Fig. 1 shows the TEM micrographs of DPPI-NPs by reverse microemulsion method with definite concentration of surfactant but different water to surfactant molar ratio (*R*). The particles appear spherical with a fairly low polydispersity. The average particle size decreases upon increasing *R*. At low *R*, the microemulsion droplet size is smaller, and hence the number of TEOS molecules partitioned at the interface of the surfactant and water is less. As a result, there are a smaller number of monomers and nuclei formed. Further, conditions of bound water and rigid interface due to close packing of surfactant molecules make the mobility of these monomers less, decreasing the intermicellar exchange. These conditions make the environment conducive for less nuclei formation and a more enhanced growth rate. Hence the terminal particle size is larger. As the *R* increases, the droplet size of the microemulsion increases and more of the TEOS molecules are hydrolyzed at the interface. Also the partition coefficient of TEOS increases with size of droplet and the intermicellar exchange rate increases due to a decrease in the rigidity of the surfactant film. Under these conditions, the rate of

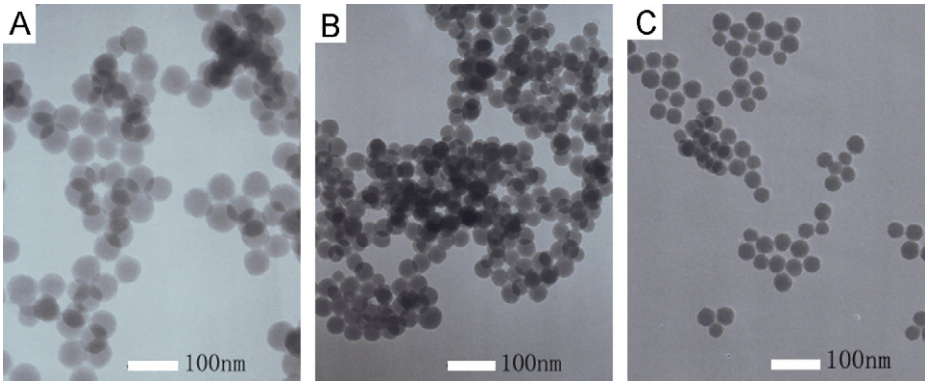

Fig. 1. TEM images of DPPI-NPs prepared by reverse microemulsion method with different water to surfactant molar ratio: (A) $R = 6{:}1$, $D_{av} = 54$ nm, CV = 7%; (B) $R = 10{:}1$, $D_{av} = 37$ nm, CV = 6%; and (C) $R = 14{:}1$, $D_{av} = 29$ nm, CV = 9%. D_{av} is the average particle size. CV is coefficient of variation. The inset bar is 100 nm.

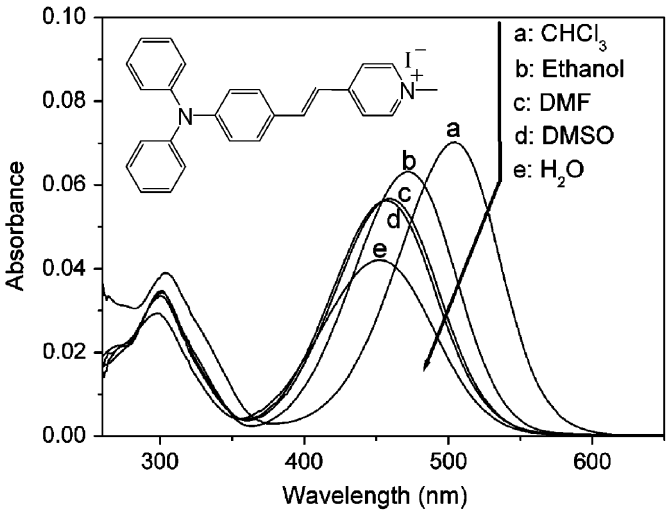

Fig. 2. Absorption spectra of DPPI in various solvents (10^{-6} M).

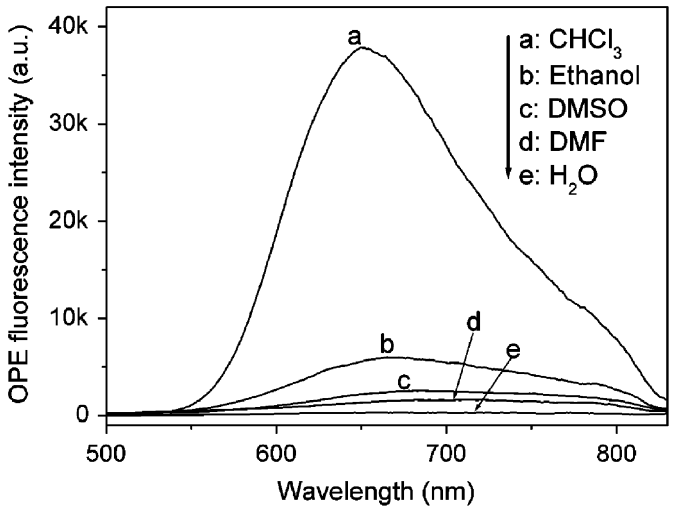

Fig. 3. OPE fluorescence spectra of DPPI in various solvents (10^{-5} M) excited at the absorption maximum (Abs_{max}) of each sample.

intramicellar nucleation increases and the resultant particle size is smaller [26]. More effects of reaction conditions on the particle size were reported elsewhere [27].

3.2. Photophysical properties of free dye solutions of DPPI

Dilute dye solutions of DPPI, as low as 10^{-6} M, were prepared for absorption measurements in order to avoid aggregation effect. A blue shift was observed in the absorption maxima of DPPI with increasing polarity of the solvent, being most pronounced in water (54 nm) compared to chloroform (Fig. 2). The change trend is consistent with the reported conclusion of other zwitterionic hemicyanine dyes [28–30]. An illustration of solvent effect on the absorption process is shown in Section 3.3.

Fig. 3 presents the OPE fluorescence spectra of 10^{-5} M DPPI in the following solvents: chloroform, ethanol, DMF, DMSO, and water. All the spectrum behaviors are similar to the reported features of zwitterionic hemicyanine dyes [29,30]. First, DPPI is highly susceptible to solvent polarity. Second, the fluorescence spectra show red shift with an increase in the solvent polarity except DMF. The emission is intense in chloroform but rapidly decreases as the solvent polarity increases. Considering that DPPI is a push-pull type compound (an electron-donating diphenyl amino group at one end and an electron-withdrawing pyridinium group at the other end) with rotatable C–N single bond, above fluorescent behaviors can be ascribed to "twisted intramolecular charge transfer" (TICT) upon excited state [31]. TICT is a process of intramolecular transfer from the donor to the acceptor upon excited state accompanied by twisted structure geometry. It is much less emissive and strongly dependent on the polarity of solvent. An increase in the polarity of solvent can decrease the activation barrier and enhance the TICT process. This is responsible for the red shift and rapidly reduced fluorescence intensity in polar solvent. The exception of the lower fluorescence intensity in DMF than that in DMSO is probably due to the large quantity of dissolved oxygen in DMF, which causes enhanced non-radiative decay of the excited state [32–34]. Using Bom–Marcus-type theory, Fromherz has rationalized the solvatochromism of blue-shifted absorption and red-shifted emission of hemicyanine dyes with increasing polarity of solvent [30].

The concentration effect on the OPE fluorescence spectra of DPI was studied in ethanol solutions with following dye concentrations: 10^{-6}, 10^{-5}, 4×10^{-5}, and 10^{-3} M. The recorded OPE fluorescence spectra are shown in Fig. 4. It is noted that obvious fluorescence quenching behavior occurs, especially for the high concentration of 10^{-3} M. Main reason can be ascribed to the aggregation and collision quenching between dye molecules as reported elsewhere [32,35,36]. The OPE fluorescence of DPPI is very sensitive to the dye concentration since fluorescence quenching occurs at a relatively low concentration of 4×10^{-5} M.

3.3. Photophysical properties of DPPI-NPs

All the DPPI-NPs used for spectroscopic measurements were the type of 29 nm in the average particle size. Fig. 5 shows the absorption spectra of 0.1 mg/mL DPPI-NPs dispersions in various solvents. Absorptions of blank suspensions were recorded for comparison. The scattering effect is very weak in the range of 420–600 nm, so its contribution to the absorption of DPPI-NPs can be considered negligible in this range. The absorption behaviors of DPPI-NPs were similar to those of free dye solutions. This allowed an estimation of the dye content in DPPI-NPs (η) by absorption measurements. Table 1 lists the overall dye concentrations (C) of 0.1 mg/mL DPPI-NPs dispersions and the corresponding η in DPPI-NPs for each solvent. The values are close to each other, indicating that it is a reliable method to calculate η in NPs. Here, the average value of the η in various solvents, 0.23% based on the mass of NPs, was considered as the true η in DPPI-NPs.

For 2 mg/mL DPPI-NPs dispersions, the overall dye concentration is calculated as 0.93×10^{-5} M, which is comparative to 10^{-5} M of the free dye solutions. The OPE fluorescence intensity of DPPI-NPs dispersions generally remains with a tiny decrease upon the increasing solvent polarity. Fig. 6 compares the OPE fluorescence spectra of DPPI-NPs dispersion and free dye solutions in ethanol and water. The OPE fluorescence at peak wavelength (Em_{max}) of DPPI-NPs dispersions are much stronger than that of free DPPI solutions, especially in highly polar water (about 94 times enhanced). More values of fluorescence intensity ratio at their peak wavelengths (R_I) are summarized in Table 1. In addition, it is observed that the OPE fluorescence peak of the DPPI-NPs shows red shift as the polarity of solvent increases, which is similar to that of free dye solutions (Table 1). Which is different is that Em_{max} is much shorter and the extent of

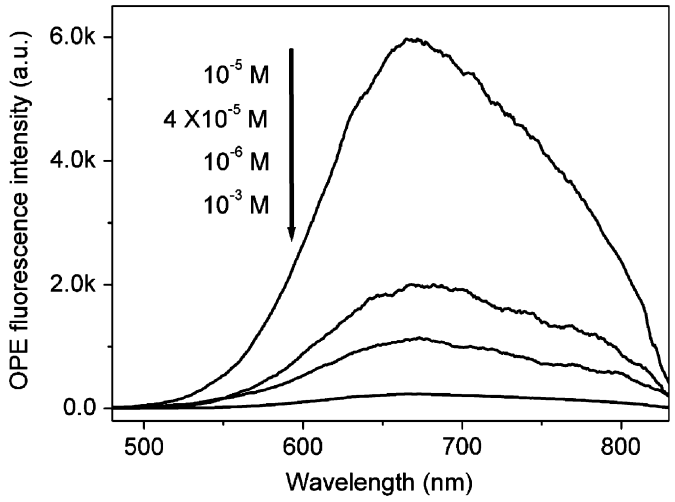

Fig. 4. OPE fluorescence spectra of DPPI in ethanol with different dye concentrations. Emission scans were collected by exciting at 472 nm.

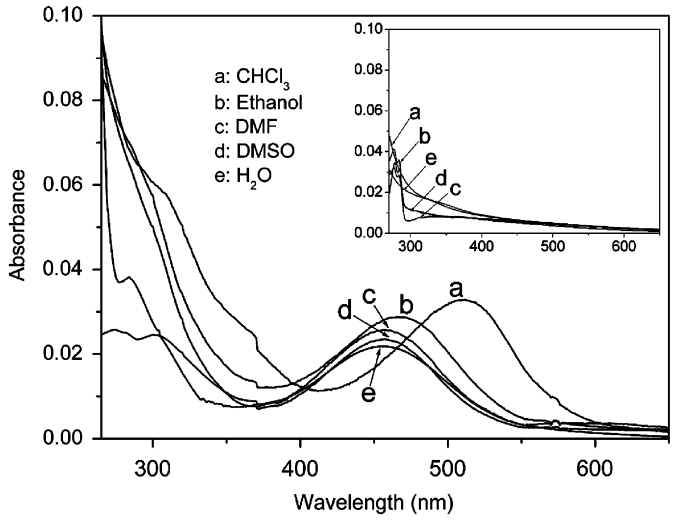

Fig. 5. Absorption spectra of DPPI-NPs and blank silica NPs (inset graph) in various solvents (0.1 mg/mL).

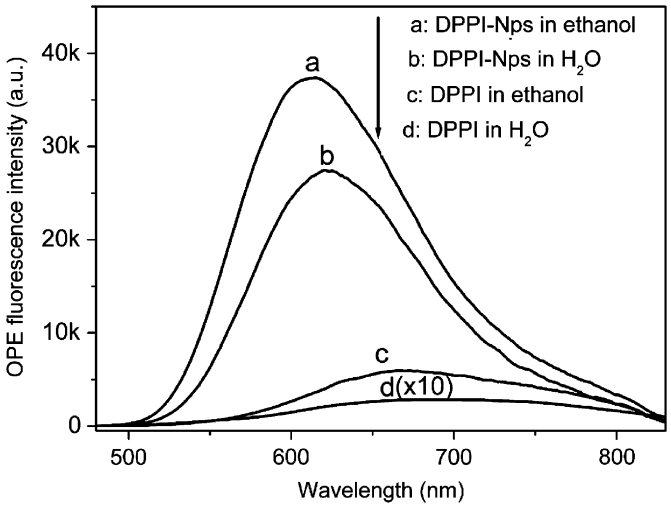

Fig. 6. OPE fluorescence spectra of DPPI-NPs and DPPI in ethanol and water. Excitation was at Abs_{max} of each sample. The OPE fluorescence intensity of DPPI in water has been 10 times magnified to bring into scale.

Table 1
Dye contents and spectral properties of DPPI-NPs dispersions.

Solvent	DDPI-NPs dispersion			DPPI solution		
	C ($\times 10^{-6}$ M)	η (wt%)	Em_{max} (nm)	C_{max}[a] ($\times 10^{-3}$ M)	Em_{max} (nm)	R_I
$CHCl_3$ (4.81[b])	0.467	0.23	609	~0.05	651	1.3
Ethanol (24.5[b])	0.450	0.22	613	~7.3	666	6.3
DMF (36.7[b])	0.452	0.22	617	~32	682	19
DMSO (46.7[b])	0.429	0.21	619	~76	685	13
H_2O (80.1[b])	0.527	0.26	622	~1.7	692	94
	0.465[c]	0.23[c]	–			–

[a] The maximum concentration (C_{max}) of DPPI in solvents at room temperature.
[b] The dielectric constant of solvent at 20 °C taken from Ref. [44].
[c] The calculated average values of C and η.

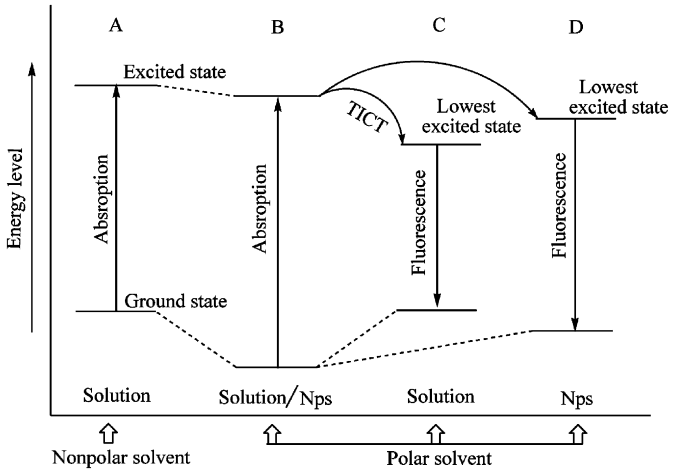

Fig. 7. Energy level changes of absorption and fluorescence processes in different environments.

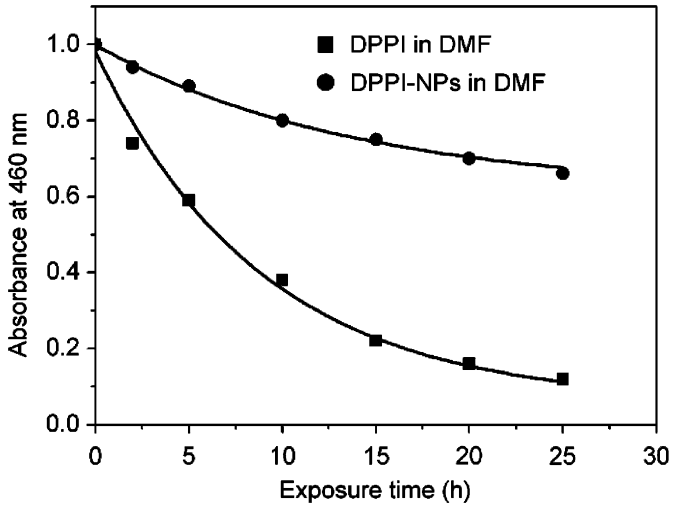

Fig. 8. Comparison of photostability of the free DPPI solution and DPPI-NPs dispersion. The decay curves of absorbance were plotted as a function of the time of samples being exposed under 254-nm UV illumination.

red shift is much smaller. The results indicate that solvent effect on fluorescence also exists in the DPPI-NPs dispersions. On the basis of porosity of silica NPs [7,22], we believe that solvent molecules can penetrate into the silica matrix to extent. Hence, the solvent effect still influences the ground and excited states as that in free dye solution (Fig. 7, from A to B). Our hypothesis is supported by the similarity in the absorption spectra of DPPI-NPs dispersions and free dye solutions in various solvents (Figs. 2 and 5).

Fluorescence can be considered as the reverse process of absorption. As discussed above, the excited state of free DPPI solution formed after absorption would relax to the lowest excited state by a TICT process (Fig. 7, from B to C). An increasing solvent polarity can lead to an enhanced TICT process and causes larger energy loss of the excited state [37,38]. In the case of DPPI-NPs dispersions, dye molecules are trapped inside the silica matrix, as a result of which the rotation, vibration, and formation of excimer are largely restricted [39–42]. Under the circumstance, TICT process is inhibited despite of solvent effect on DPPI-NPs dispersions. Thus, there is reduced energy loss of excited state and larger energy difference between the lowest excited state and the corresponding ground state (Fig. 7, from B to D), which lead to blue-shifted emission bands for DPPI-NPs dispersions compared to free dye solutions. In addition, restricted TICT process limits the non-radiative decays [43], so DPPI-NPs possess much more intense fluorescence (Fig. 6). It is also noted that there is small red shift in the fluorescence spectra of DPPI-NPs, which gives another evidence of that solvent effect on fluorescence spectra exists but is largely weakened in DPPI-NPs. To get more insight into the solvent effect on the fluorescence of DPPI-NPs, we conducted the experiments of fluorescence spectra against time for DPPI-NPs dispersions stored in the dark. It was observed that the fluorescence spectra generally remained for a long period of two weeks. Since the fluorescence of dye molecules is much weaker in solution than that in silica NPs, the generally remained fluorescence indicates that little dye leakage occurred in DPPI-NPs dispersions.

In the case of 2 mg/mL DPPI-NPs dispersions, a characteristic should be noted is that all the dye molecules are restricted in a few silica NPs and the dye concentrations are high up to 1.02×10^{-2} M (calculated with the silica density of 2 g/mL [1]). No fluorescence quenching (Fig. 6) as that in ethanol solution (Fig. 4) was observed. This may be due to the effective immobility and segregation of dye molecules by silica matrix, which largely restrict the collision of dye molecules and the formation of excimer at high dye concentration.

To investigate the photostability of DPPI-NPs, we also performed photobleaching experiments to compare the relative stabilities of the free dye and the DPPI-NPs. Photobleaching of a luminophore is often caused by a photooxidation reaction. DMF usually contains a large quantity of dissolved oxygen, so no treatment for supplying oxygen into the solution was required if samples in DMF were used for comparison. Samples of 10^{-5} M dye solution and 2 mg/mL DPPI-NPs in DMF were prepared at the same time for comparison. 200 μL portions of above samples were exposed under 254-nm UV illumination from a 100 w UV lamp. The absorbance at 460 nm and OPE fluorescence intensity at peak-wavelength were recorded as a function of exposure time. Fig. 8 illuminates the decay curves of absorbance at 460 nm as a function of exposure time for DPPI solution in DMF and DPPI-NPs dispersion in DMF. The absorbance of the free dye solution fall to 11% of it initial value after 25 h, while 68% of its initial value was retained in the case of DPPI-NPs. Similar result was observed for the OPE fluorescence of the two samples. No fluorescence of the free dye solution was observed after exposing to UV light for 10 h. However, the fluorescence intensity of DPPI-NPs mainly remained with a loss of about 20%. Obviously, silica encapsulation largely improves the photostability of dye molecules under continuous excitation. The main cause may be that silica matrix can effectively exclude the oxygen outside [45]. Above all, silica matrix provides good protection of dye molecules and improves the luminescent intensity and photostability.

3.4. TPE fluorescence and cellular uptake of DPPI-NPs

Fig. 9 shows the TPE fluorescence spectra of DPPI-NPs dispersions and DPPI free solutions with comparative overall dye concentration under 800-nm excitation. TPE fluorescence of DPPI-NPs dispersions were found of similar spectroscopic characteristic with OPE fluorescence, such as the shape of fluorescence spectra, close position of emission peak, and much stronger fluorescence intensity compared to free dye solutions. The result indicates that OPE and TPE fluorescence process the same excited state. Two reasons may contribute to the enhanced TPE fluorescence in DPPI-NPs dispersions. One is that the local dye

concentration in DPPI-NPs is very high (1.02×10^{-2} M), which is favored by the nonlinear two-photon absorption and excitation. The other is that silica matrix protects the dye molecules from the fluorescence quenching as described for OPE fluorescence.

The cellular uptake of DPPI-NPs was evaluated by fluorescence microscope. Fig. 10 illustrates the TPE fluoresce imaging of Hela cells incubated with a 0.08 mg/ml DPPI-NPs aqueous dispersion for 2 h. Significant cellular staining with accumulation of the NPs in the cytoplasm and membranes was observed (though the exact mechanism is not clear at this point, it is probably endocytosis), as reported elsewhere [7,18]. It indicates that the DPPI-NPs have potential application in TPA bio-imaging. The cytotoxcity of DPPI-NPs was determined by MTT assay. Fig. 11 presents the number of cell survival after 2 h incubation of DDPI-NPs. Results reveal that the presence of DPPI-NPs slightly affects cell viability. Further work involving surface modification and attachment of the DPPI-NPs to biomolecules for biological applications is currently being carried out in our laboratory.

4. Conclusions

Silica NPs encapsulating a TPA dye of DPPI have been prepared without any chemical modification of the dye molecule. The prepared DDPI-NPs possess narrow size distributions and the particle size can be tuned by changing the water to surfactant molar ratio in the reaction. The solvent effect on the absorption spectra of DPPI-NPs dispersions is similar to that of free dye solutions, indicating that solvents can partly penetrate into the silica matrix and contact the DPPI molecules. With increasing solvent polarity, large red shift and rapidly reduced OPE fluorescence intensity in free DPPI solutions were efficiently inhibited by the protection of silica matrix in DPPI-NPs dispersions. DPPI-NPs dispersions emit obvious TPE fluorescence upon 800-nm excitation, which was, however; too weak to be detected in DPPI free solutions. Using two-photon laser scanning fluorescence microscopy, it is observed that the DPPI-NPs can be actively uptaken by Hela cells and localized in the cytoplasm and membrane. The good dispersibility, intense OPE and TPE fluorescence,

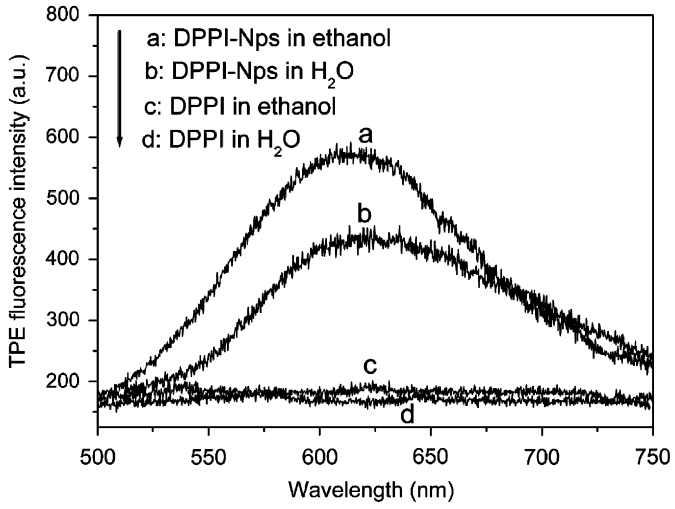

Fig. 9. TPE fluorescence spectra of DPPI-NPs dispersion (2 mg/mL) and DPPI solutions (10^{-5} M) in ethanol and water. The excitation wavelength was 800 nm.

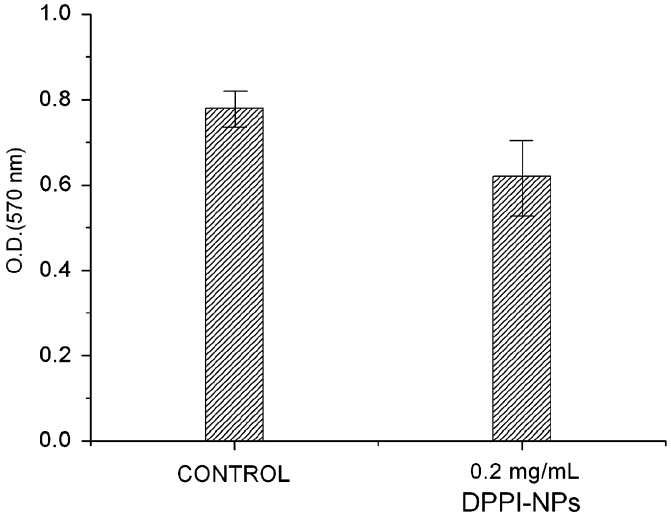

Fig. 11. Viability of Hela cells after incubation with DPPI-NPs for 2 h and MTT treatment (values: mean ± standard deviation).

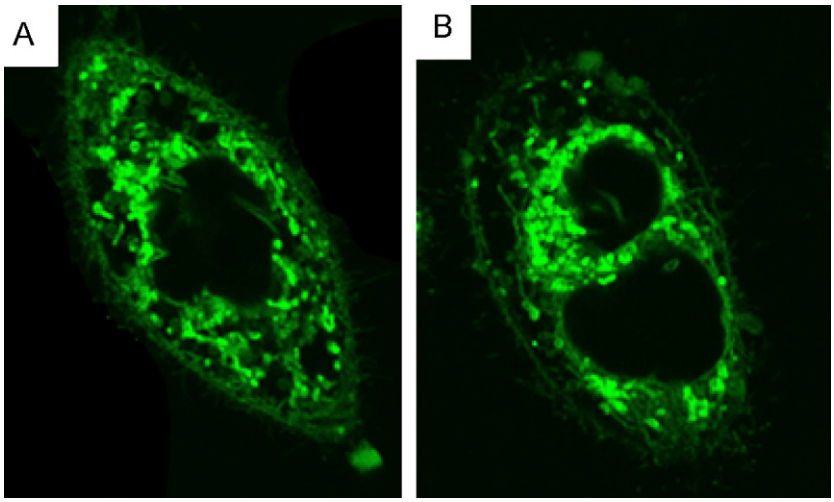

Fig. 10. TPE fluorescence images of a single living cell (A) and a cell in division (B), stained with DPPI-NPs. The excitation wavelength is 800 nm.

the ability of penetrating cells, and low cytotoxcity reveal that DPPI-NPs have potential application in biomedical fields.

Acknowledgments

The authors would like to thank Dr. Ao for kind help. The support of this work by High Technology Research Plan of Jiangsu Province (BG2006006) and National High-Tech Research and Development Plan (2006AA03Z313).

References

[1] A. van Blaaderen, A. Vrij, Langmuir 8 (1992) 2921–2931.
[2] X.J. Zhao, R.P. Bagwe, W.H. Tan, Adv. Mater. 16 (2004) 173–176.
[3] W.L. Vos, R. Sprik, A. van Blaaderen, A. Imhof, A. Lagendijk, G.H. Wegdam, Phys. Rev. B 53 (1996) 16231–16235.
[4] L. Wang, W.H. Tan, Nano Lett. 6 (2006) 84–88.
[5] R. He, X.G. You, J. Shao, F. Gao, B.F. Pan, D.X. Cui, Nanotechnology 18 (2007) 315601.
[6] X.J. Zhao, R. Tapec-Dytioco, K.M. Wang, W.H. Tan, Anal. Chem. 75 (2003) 3476–3483.
[7] I. Roy, T.Y. Ohulchanskyy, H.E. Pudavar, E.J. Bergey, A.R. Oseroff, J. Morgan, T.J. Dougherty, P.N. Prasad, J. Am. Chem. Soc. 125 (2003) 7860–7865.
[8] P. Sharrna, S. Brown, G. Walter, S. Santra, B. Moudgil, Adv. Colloid Interface 123 (2006) 471–485.
[9] S. Santra, J.S. Xu, K.M. Wang, W.H. Tan, J. Nanosci. Nanotechnol. 4 (2004) 590–599.
[10] W.R. Zipfel, R.M. Williams, W.W. Webb, Nat. Biotechnol. 21 (2003) 1368–1376.
[11] H.M. Kim, X.Z. Fang, P.R. Yang, J.-S. Yi, Y.-G. Ko, M.J. Piao, Y.D. Chung, Y.W. Park, S.-J. Jeon, B.R. Cho, Tetrahedron Lett. 48 (2007) 2791–2795.
[12] T. Gura, Science 276 (1997) 1988–1990.
[13] M. Albota, D. Beljonne, J.-L. Brédas, J.E. Ehrlich, J.-T. Fu, A.A. Heikal, S.E. Hess, T. Kogej, M.D. Levin, S.R. Marder, D. McCord-Maughon, J.W. Perry, H. Röckel, M. Rumi, G. Subramaniam, W.W. Webb, et al., Science 281 (1998) 1653–1656.
[14] B.A. Reinhardt, L.L. Brott, S.J. Clarson, A.G. Dillard, J.C. Bhatt, R. Kannan, L. Yuan, G.S. He, P.N. Prasad, Chem. Mater. 10 (1998) 1863–1874.
[15] O. Mongin, L. Porrés, L. Moreaux, J. Mertz, M. Blanchard-Desce, Org. Lett. 4 (2002) 719–722.
[16] X.M. Wang, Y.F. Zhou, G.Y. Zhou, W.L. Jiang, M.H. Jiang, Bull. Chem. Soc. Jpn. 75 (2002) 1847–1854.
[17] J.L. Yan, M.C. Estévez, J.E. Smith, K.M. Wang, X.X. He, L. Wang, W.H. Tan, Nanotoday 2 (2007) 44–50.
[18] M. Lal, L. Levy, K.S. Kim, G.S. He, X. Wang, Y.H. Min, S. Pakatachi, P.N. Prasad, Chem. Mater. 12 (2000) 2632–2639.
[19] L. Levy, Y. Sahoo, K.-S. Kim, E.J. Bergey, P.N. Prasad, Chem. Mater. 12 (2002) 3715–3721.
[20] S. Kim, H.E. Pudavar, P.N. Prasad, Chem. Commun. (2006) 2071–2073.
[21] S. Kim, T.Y. Ohulchanskyy, H.E. Pudavar, R.K. Pandey, P.N. Prasad, J. Am. Chem. Soc. 129 (2007) 2669–2675.
[22] L. Bertazza, L. Celotti, G. Fabbrini, M.A. Loi, M. Maggini, F. Mancin, S. Marcuz, E. Menna, M. Muccini, U. Tonellato, Tetrahedron 62 (2006) 10434–10440.
[23] G.A. Lawrie, B.J. Battersby, M. Trau, Adv. Funct. Mater. 13 (2003) 887–896.
[24] X.M. Wang, C. Wang, W.T. Yu, Y.F. Zhou, X. Zhao, Q. Fang, M.H. Jiang, Can. J. Chem. 79 (2001) 174–182.
[25] R.P. Bagwe, K.C. Khilar, Langmuir 16 (2000) 905–910.
[26] F.J. Arriagada, K. Osseo-Asare, Colloids Surf. A 154 (1999) 311–326.
[27] R.P. Bagwe, C.Y. Yang, L.R. Hilliard, W.H. Tan, Langmuir 20 (2004) 8336–8342.
[28] R.A. Hall, P.J. Thistlethwaite, F. Grieser, N. Kimizuka, T. Kunitake, Langmuir 10 (1994) 2743–2747.
[29] C.F. Zhao, R. Gvishi, U. Narang, G. Ruland, P.N. Prasad, J. Phys. Chem. 100 (1996) 4526–4532.
[30] P. Fromherz, J. Phys. Chem. 99 (1995) 7188–7192.
[31] Q. Song, C.E. Evans, P.W. Bohn, J. Phys. Chem. 97 (1993) 13736–13741.
[32] J.R. Lakowicz, Principles of Fluorescence Spectroscopy, Plenum, New York, 1999.
[33] J. Saltiel, B.W. Atwater, in: G.S. Hammond (Ed.), Advances in Photochemistry, vol. 14, Wiley-Interscience, New York, 1987.
[34] U. Graf, H. Niikura, S. Hirayama, J. Phys. Chem. A 101 (1997) 1292–1298.
[35] E.M. Ebeid, S.T. Abdel-Halim, M.H. Abdel-Kader, J. Phys. Chem. 92 (1988) 7255–7257.
[36] G.Z. Chen, Z.Q. Huang, Z.Z. Zheng, Fluoroimmunoassay, Science Press, Beijing, 1990.
[37] S. Nad, M. Kumbhakar, H. Pal, J. Phys. Chem. A 107 (2003) 4808–4816.
[38] X. Cao, R.W. Tolbert, J.L. McHale, W.D. Edwards, J. Phys. Chem. A 102 (1998) 2739–2748.
[39] R. Sabate, M. Gallardo, J. Estelrich, J. Colloid. Interface Sci. 233 (2001) 205–210.
[40] D. Avnir, V.R. Kaufman, R. Reisfeld, J. Non-Cryst. Solids 74 (1985) 395–406.
[41] P. Das, A. Chakrabarty, A. Mallick, N. Chattopadhyay, J. Phys. Chem. B 111 (2007) 11169–11176.
[42] B.P. Wittmershaus, J.J. Skibicki, J.B. McLafferty, Y.-Z. Zhang, S. Swan, J. Fluor. 11 (2001) 119–128.
[43] Y. Huang, T. Cheng, F. Li, C. Luo, C.-H. Huang, Z. Cai, X. Zeng, J. Zhou, J. Phys. Chem. B 106 (2002) 10031–10040.
[44] N.L. Chen, Solvent Handbook, third ed., Chemical Industry Press, Beijing, 2002.
[45] W. Lian, S.A. Litherland, H. Badrane, W.H. Tan, D.H. Wu, H.V. Baker, P.A. Gulig, D.V. Lim, S.G. Jin, Anal. Biochem. 334 (2004) 135–144.